scientific reports

Check for updates

OPEN

Enhancing fresh-cut spinach preservation with carbon quantum dot-based composite coatings

Sijing Zhu[1], Linxuan Jin[1], Yueyue Zhang[1], Feiping Chen[2], Amr Farouk[3], Tao Yang[4], Guohui Yi[4], Houxue Li[5], Zhao-Jun Ban[1] & Lingling Liu[1]✉

In order to address the issue of fresh-cut vegetable waste, this research was done on postharvest preservation techniques using carbon dots (CDs) and sericin protein (SC) composite coatings (SCCD). SCCD was synthesized using ultrasound technology, exhibiting promising antioxidant and antibacterial activities. The influence of CDs concentration variations on the morphological, fluorescence quenching, UV-shielding, and structural properties of SCCD was comprehensively investigated. Protein quenching caused by endogenous fluorescence was lessened by the interaction of SC and CDs. The inhibition zones grew from 7.8 to 19.21 mm and 20.01 mm, respectively, and the antibacterial activity of SCCD-1.0 rose by 146% (for *B. subtilis*) and 157% (for *E. coli*) in comparison to the SC. Additionally, the SCCD composite coating successfully delayed colonies expansion, preserved spinach flavor, decreased the fresh-cut spinach's weight loss rate and malondialdehyde concentration in the storage experiment by 41.67% and 42.11%, respectively. These findings support the SCCD composite coating's potential as an active food packaging material.

Keywords Sericin, Carbon dot, Composite coatings, Vegetables preservation

With the rapid development of contemporary social economy and technology, pre-made vegetable dishes now account for 22% of urban dietary intake, reflecting their growing importance. Fresh-cut vegetables are in great demand owing to their freshness, nutrition, convenience, and safety[1]. Fresh vegetables is also essential to improve the quality of your diet, prevent chronic diseases, achieve healthy bowel habits, and stay healthy[2]. However, attributing to tissue damage and inappropriate storage methods during pretreatment, nutrition and quality in fresh-cut vegetable will diminish quickly, and excessive consumption of ultra-processed foods has been shown to lead to intestinal motility disorders. Postharvest nanocomposite coating technology is a new type of preservation method, which is fabricated from edible materials with function of coating the food to increase the natural barrier for protection[3], maximizing shelf life and maintaining quality of fresh fruits and vegetables through minimal processing[4]. Not only does the nanocomposite coating have the advantages of inhibiting bacteria, delaying fruit senescence, enhancing fruit hardness, soluble solids, but it is also easier to degrade than traditional packaging materials such as plastics[5], therefore this nanomaterial composite coating have been progressively produced and used in recent years. Wang et al.[6] used visible light-responsive chitosan/sodium alginate/QDs@ZIF-8 nanocomposite films to preserve kiwifruit, which have antibacterial and ethylene scavenging performance; Xin et al.[7] applied whey protein-based emulsion membrane treatment for fresh-cut apple preservation; Hou et al.[8] developed an edible and easy-to-wash D-Limonene nanoemulsion film and used it for the preservation of bananas.

Biodegradable packaging commonly utilizes proteins, lipids, polysaccharides, and biological antibacterial agents as raw materials. One such material is sericin (SC), a water-soluble polymer protein derived from the silkworm[9]. SC is extensively utilized in nanocomposite membranes because of its biodegradability, biocompatibility, minimal environmental contamination, and its ability to easily absorb and release in water[6,10]. Regrettably, the inherent limitations of biopolymer materials, such as their restricted UV shielding, mechanical

[1]School of Biological and Chemical Engineering, Zhejiang University of Science and Technology, Zhejiang Provincial Key Laboratory of Chemical and Biological Processing Technology of Farm Products, Hangzhou 310023, China. [2]Sericultural & Agri-Food Research Institute Guangdong Academy of Agricultural Sciences/Key Laboratory of Functional Foods, Ministry of Agriculture and Rural Affairs/Guangdong Key Laboratory of Agricultural Products Processing, Guangzhou 510610, China. [3]Flavor and Aroma Chemistry Department, National Research Centre, Dokki, Cairo 12622, Egypt. [4]School of Pharmacy, Hainan Provincial Key Laboratory for Research and Development of Tropical Herbs, Hainan Medical University, Haikou 571199, China. [5]Ningxia Xianfeng Agricultural Development Co., Ltd, Yinchuan 750200, China. ✉email: llliu@zust.edu.cn

strength, and resistance to oxidation and microorganisms, hinder their widespread application in food packaging. Therefore, the combined effect of two components is considered to augment the role of nanomaterial composite coating in food preservation.

A type of spherical, zero-dimensional nanomaterials having a diameter of less than 10 nm have been referred to as carbon dots (CDs). When single-walled carbon nanotubes (SWNTs) were prepared by XU and others in 2004 using the arc discharge method, a fluorescent carbon nanoparticle—later known as the carbon quantum dot—was separated from the crude soot[11]. After that, this subject has attracted significant interest and research due to its capacity to tune luminescence wavelength, simplicity of modifying surface functionality, and strong biocompatibility. Researchers have proved the effectiveness of carbon dot food packaging in the field of food preservation through a number of tests conducted both domestically and internationally. Wang and his colleagues[12] developed films made of a combination of CDs/CS nanocomposites derived from pleurotus eryngii. These films were then applied to fresh-cut pears preservation successfully. Du and He[13] investigated a composite material consisting of zinc-doped carbon quantum dots and chlorogenic acid (Zn-CQDs/CGA). This composite was found to effectively inhibit browning and preserve the quality of longan fruit. Fan and colleagues[14] studied the use of carbon dots coated with chitosan to improve the storage quality of fresh-cut cucumber by affecting microorganisms. Carbon dots (CDs) show promising potential for food preservation applications as they can serve as key components in multifunctional bio-composite coatings, exhibiting antibacterial, antioxidant, UV-shielding, and pH-sensing properties.

Spinach is a green leafy vegetable, low in calories and containing rich essential micronutrients (vitamin A, vitamin C, and iron) that are highly valued in international markets. However, due to the large leaf area and wide distribution of stomata in spinach, it is very susceptible to spoilage fungus infection and it is not resistant to storage[15]. Therefore, this experiment chose spinach as the research object to explore a suitable preservation method to extend the shelf life of fresh-cut spinach.

This study used banana peels as materials because they are excellent for sustainable CD synthesis due to their high carbohydrate content (59–76%). As an inedible agricultural waste, banana peels also help repurpose resources[16]. Ultrasound technology was employed to synthesize a novel sericin-carbon dot (SCCD) nano-composite coating material. The objective was to address challenges that fresh-cut vegetables tend to deteriorate after harvest due to physiological metabolic activities. The properties of these composite particles and the interaction between SC and CDs were investigated to understand the binding mechanism and factors influencing the composite coating material. Furthermore, the antibacterial efficacy of the nano-composite coating material was evaluated through studies assessing its ability to inhibit the growth of common bacteria, confirming its potential for food preservation. Subsequently, the nano-composite coating material was applied to fresh spinach and stored at a commercial temperature of 4 °C. Quality-related attributes such as visual appearance, texture, and nutritional composition were monitored throughout the storage period. These methodologies and experiments aim to devise innovative technical solutions for combating food waste and offer valuable insights and references for further research and practical applications in the realm of food preservation.

Materials and methods

Materials

Bananas and spinach were bought from local market in Hangzhou, China. Sericin protein powder was bought from Peptide Biotechnology Co., Ltd (Xi'an, China). All chemical agents were analytical grade and used without further purification unless otherwise stated. *Escherichia coli* (ATCC8739) and *Bacillus subtilis* (ATCC6633) were obtained from the College of Biological and Chemical Engineering laboratory C2-413 (Hangzhou, China).

Preparation of cds

Carbon dots were prepared according to Sul et al.[16] with modifications using banana peel as a carbon precursor. A juice extractor (Ningbo Lafanu Household Electrical Appliances Co., Ltd., Zhejiang, China) was used to homogenize a 20 g sample of cleaned banana peel with distilled water at a 1:5 (w/v) ratio. Following being heated to 180 °C for eight hours, the mixture was placed in a hydrothermal reaction kettle and allowed to cool to room temperature. After obtaining the solution, it was ultrasounded in KQ-300DE ultrasonic device (Kunshan Ultrasonic Instrument Co., Ltd., Jiangsu, China) at 25 °C and 300 Hz ultrasounded for 40 min. The supernatant underwent two days of dialysis after being filtered twice through a 0.22 μM filter membrane to eliminate insoluble particles. The CDs solution from banana peel is found in the filtered supernatant.

Preparation of the SCCD composite coating

The SC solution (10 mg/mL) was prepared by dispersing the freeze-dried SC powder into deionized water under stirring conditions. CDs solution was added to the SC solution, resulting mixed ultrasounded in KQ-300DE ultrasonic device (Kunshan Ultrasonic Instrument Co., Ltd., Jiangsu, China) was for 40 min at 25 °C and 300 Hz to prepare SCCD (the concentration is 0 mg/mL, 2 mg/mL, 4 mg/mL, 6 mg/mL, 8 mg/mL and 10 mg/mL, respectively).

Morphology and size distribution of CDs

The morphology of CDs was analyzed with a transmission electron microscope (TEM) at 200 kV. Applying dynamic light-scattering with a Zetasizer Nano ZS with a 4 mW He–Ne laser (633 nm wavelength) at 25 °C, the size distribution of CDs was ascertained.

Characterization of the SCCD composite coating

Morphology and particle size distribution

Utilizing a 200 kV transmission electron microscope (HT7800, Hitachi High-Technologies Japan), the morphology of 10 mg/mL SCCD was examined. Dynamic light scattering (DLS) was used to find the average diameter (Dz), size distribution of the particles and polydispersity index (PDI). This was done on a Zetasizer Nano-ZS device (Malvern Instruments Ltd., Malvern, Worcestershire, UK) with a 4 mW He–Ne laser (633 nm wavelength) at 25 °C[17], the size distribution of SCCD nanosolution (0 mg/mL, 2 mg/mL, 4 mg/mL, 6 mg/mL, 8 mg/mL and 10 mg/mL) was ascertained.

Fourier transforms infrared (FT-IR)

The chemical structure of the 10 mg/mL SC, CDs, 10 mg/mL SCCD were measured using an FT-IR spectrometer (BRUKER V70, Bruker Inc., Germany) in transmittance mode. The spectrometer had a scan resolution of 4 cm^{-1} and a scanning range of 4000–400 cm^{-1}.

Fluorescence quenching measurement

The contact and quenching phenomenon of the SC and SCCD (4, 6, 10 mg/mL) were quantified using protein intrinsic fluorescence spectroscopy, employing a fluorescence spectrophotometer (Hitachi F-4500, Tokyo, Japan). Fluorescence spectroscopy was conducted using an excitation wavelength of 280 nm, and the emitted fluorescence was measured within the range of 250 to 450 nm. The aperture size for both the excitation and emission was adjusted to 5 nm, while the voltage was set to 520 V. Each sample was replicated three times.

UV–Vis absorption

The UV absorption spectra of the SC and SCCD (4, 6, 10 mg/mL) were measured using a UV spectrophotometer-2600 (Shimadzu Corp., JP) at a temperature of 25 °C. The UV–Vis absorption spectra of the aqueous solution were measured within the wavelength range of 186 to 240 nm[18].

X-ray diffraction (XRD)

X-ray diffraction (XRD) was used to assess the crystal properties of particles in 10 mg/mL SC, CDs, and 10 mg/mL SCCD. The emission slit had a width of 1°, the acceptable slit had a width of 0.1 mm, and the scanning speed was 2°/min[19].

Antibacterial activity of SCCD composite coating

The inhibition effect of the SCCD system on the *E. coli* and *B. subtilis* were verified by the Oxford cup method[20]. The pure water was used as a control group. A spore suspension (0.1 mL) containing 10^5 CFU/mL of *E. coli* and *B. subtilis* were incorporated with PCA media. 0.1 mL solution (0 mg/mL, 4 mg/mL, 10 mg/mL SCCD solutions) of each was added in Oxford cups. Then *E. coli* was incubated at 37 °C for 24 h and *B. subtilis* was cultured at 37 °C for 48 h. The average inhibition zone (mm in diameter, including the diameter of the Oxford cup) was measured as the antibacterial activity of the active extracts during the triplicate trials. The Oxford cup utilized in our research had an exterior diameter of 7.80 mm.

Spinach preservation experiment

Preliminary screening

Spinach with similar size, bright color, no obvious wilting, disease and yellow leaves were selected and randomly divided into 4 groups, and sprayed by four solutions: (1) Purified water (CT), (2) 10 mg/mL sericin Protein solution (SC), (3) contained 4 mg/mL CDs in sericin protein (SCCD-0.4), (4) contained 10 mg/mL CDs in sericin protein (SCCD-1.0). Following air drying at (20 ± 1) °C, the coated sample was placed at stainless steel plates, sealed with polypropylene film and stored at temperature (4 ± 1) °C. Samples were measured in triplicate for better parallelism.

Weight loss rate

Weight loss was measured using weighing method. Spinach samples were weighed based on initial mass (W_0) and the mass at two-day intervals (W_i). Weight loss was calculated as:

$$Weight\ loss\ (\%) = \frac{W_0 - W_i}{W_0} \times\ 100\%$$

Where W_0 (g) represents the initial weight of spinach sample and W_i (g) represents the weight of spinach samples at 2, 4, 6 and 8 day.

Chlorophyll content

Chlorophyll content was tested according to Chen et al.[21]. Spinach samples (1 g) and 80% acetone (10 mL) were mixed, then centrifuged at 8000 g for 20 min. The supernatant was measured for absorbance at 645 (A_{645}) and 663 nm (A_{663}). Chlorophyll content was computed:

$$SPAD\ (g/kg) = \frac{(20.29A_{645} + 8.05A_{663}) \times\ V}{M}$$

Where A_{645} and A_{663} are the absorbance at 645 nm and 663 nm, respectively. The volume of 80% acetone for extracting the spinach juice was denoted as V (mL) and the total weight of the spinach sample was represented by the M (g).

Malondialdehyde (MDA) content

Membrane lipid peroxidation in spinach was determined by measuring malondialdehyde (MDA) content. Spinach sample (0.5 g) were homogenized in 5 mL 100 g/L of trichloroacetic acid and centrifuged at 8000 rpm for 20 min. 2 mL of the supernatant reacted with 2 mL 6.7 g/L thiobarbituric acid in a boiling water bath for 30 min. Then, the mixture was cooled rapidly on an ice bath before measuring the absorbance of the supernatant at 450 nm, 532 nm, and 600 nm. The concentration of MDA was calculated as follows:

$$MDA\,(mol/g) = \frac{[6.45 \times (A_{532} - A_{600}) - 0.56A_{450}] \times V_1 \times V_3}{V_2 \times M}$$

Where A_{450}, A_{532} and A_{600} are the absorbance at 450 nm, 532 nm and 600 nm, respectively. The total volume of reaction solution was denoted as V_1 (mL), the volume of the extracted liquid in the reaction solution was represented as V_2 (mL), and V_3 (mL) is the total volume of the extracted liquid. Additionally, the total weight of the spinach sample was represented by the M (g).

Microorganisms measurement

According to Liu et al.[20], the total amount of bacteria, mold, and yeast in spinach was measured. A 15 g spinach sample was combined with 135mL of sterile water (0.85% mass concentration), agitated for 20 min, and then serially diluted with sterile water. The cells were grown in freshly prepared media. Total bacteria were cultivated for 24 h at 37 °C on nutrient agar medium. On Potato Dextrose Agar medium, mold and yeast were cultivated for 48 h at 28 °C. Three replicates were set for each dilution gradient.

Sensory evaluation

The sensory evaluation was conducted using the methodology described by Liu et al.[20], with certain adjustments. Ten expert panelists evaluated the color, texture, odor, and appearance of the spinach after it had undergone various treatments. A sensory evaluation was conducted using a scale ranging from 0 to 5. Color (excellent/green: 5, moderate/duskiness: 3, poor/dim: 1); Odor (excellent/distinctive aroma: 5, no distinctive aroma: 3, poor/some unpleasant smell: 1); Texture (excellent/crisp: 5, moderate/crispness: 3, poor/limp: 1); Appearance (excellent/fresh appearance: 5, moderate/wilted slightly: 3; poor/no fresh appearance: 1). The average of the scores of the ten panelists is utilized to determine the sensory score for each sample, and the diversity of the sample ensures the viability of the results. Each spinach sample was randomly assigned to a set of individuals who performed an independent sensory analysis, and the scoring procedure and sequence were conducted independently and randomly to ensure reproducibility of the results.

Statistical analysis

All experimental results are obtained in at least triplicate and expressed in mean and standard deviation. The IBM SPSS Statistics 27 software was used to perform Tukey-Kramer tests where there were significant differences ($p < 0.05$) and Duncan's multiple range test for mean separation. In addition, all of the data analysis was handled by Excel 2019 and Origin 2021b software (Origin Lab Software separation Inc. Hampton, Massachusetts, USA).

Results and discussion

Characterization of the SCCD composite coating

CDs' morphology was observed by TEM imaging. The generated CDs seemed monodispersed and had a spherical shape, as observed in Fig. 1B. As shown in Fig. 1A, the size distribution of the CDs has been shown to be between 0.54 and 1.50 nm. CDs from banana were smaller than 10 nm, which is the typical size range of CDs. It was also observed by Fan[14] that CDs manufactured from kelp had a consistent quasi-spherical shape and a size distribution that ranged from 0.54 to 0.83 nm.

It is possible to observe in Fig. 2C that the color of six samples shifts from white to yellow as the concentration of CDs increases from 0 to 10 mg/ml. All of them, however, maintained a uniform and translucent look, and there were no precipitates that could be identified. The TEM micrographs (Fig. 2D) obtained subsequent to the introduction of CDs to SC particles clearly show that the resulting SCCD composites do not aggregate and retain their nanoscale size.

As can be seen in Fig. 2A-B, the SCCD nanocomposite particles that were created exhibited an average size of around 65.0 nm, which is similar in magnitude to the size of nanocomposite particles found in prior reports by Wang et al.[22] There is slight shift in the size distribution exhibited with the increase of CDs concentration. For example, the DZ in 2.0 mg/ mL was 56.0 nm, while that in 10.0 mg/mL was up to 85.3 nm. It can also be observed that SCCD-0.8 and SCCD-1.0 significantly reduces PDI (0 mg/mL: 0.402 and 10 mg/mL: 0.318), this suggests that intermolecular interaction and subsequent molecular aggregation may be triggered by an increase in CDs concentration. This allows more sericin molecules to be cross-linked with CDs to form a stable coating and the nano particle size dispersion was more uniform with the effective of CDs.

CDs, a type of nanomaterial, have strong ultraviolet (UV) absorption and can change the light's energy by absorbing certain wavelengths. The energy of ultraviolet light can be rapidly converted into heat by the high intensity light reflection and scattering that CDs produce. However, because to their great conversion properties, energy loss inevitably follows[23]. Figure 3A shows that both the pure SC solution and the composite coating samples had extremely modest spectral absorption values in the 186–240 nm range, with an absorption peak

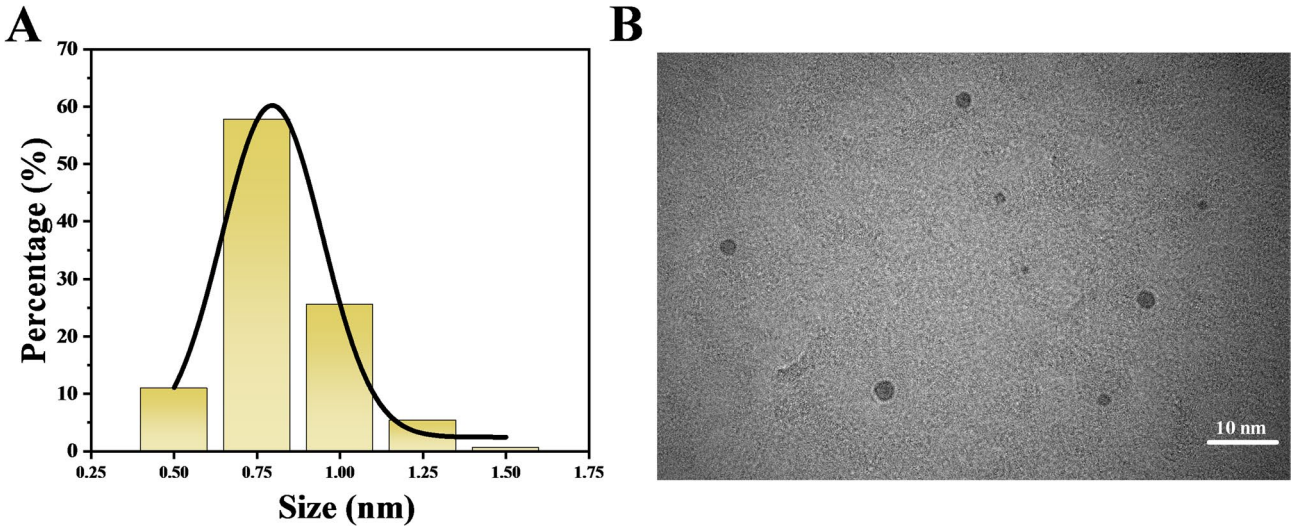

Fig. 1. (**A**) Size distribution and (**B**) TEM image of CDs.

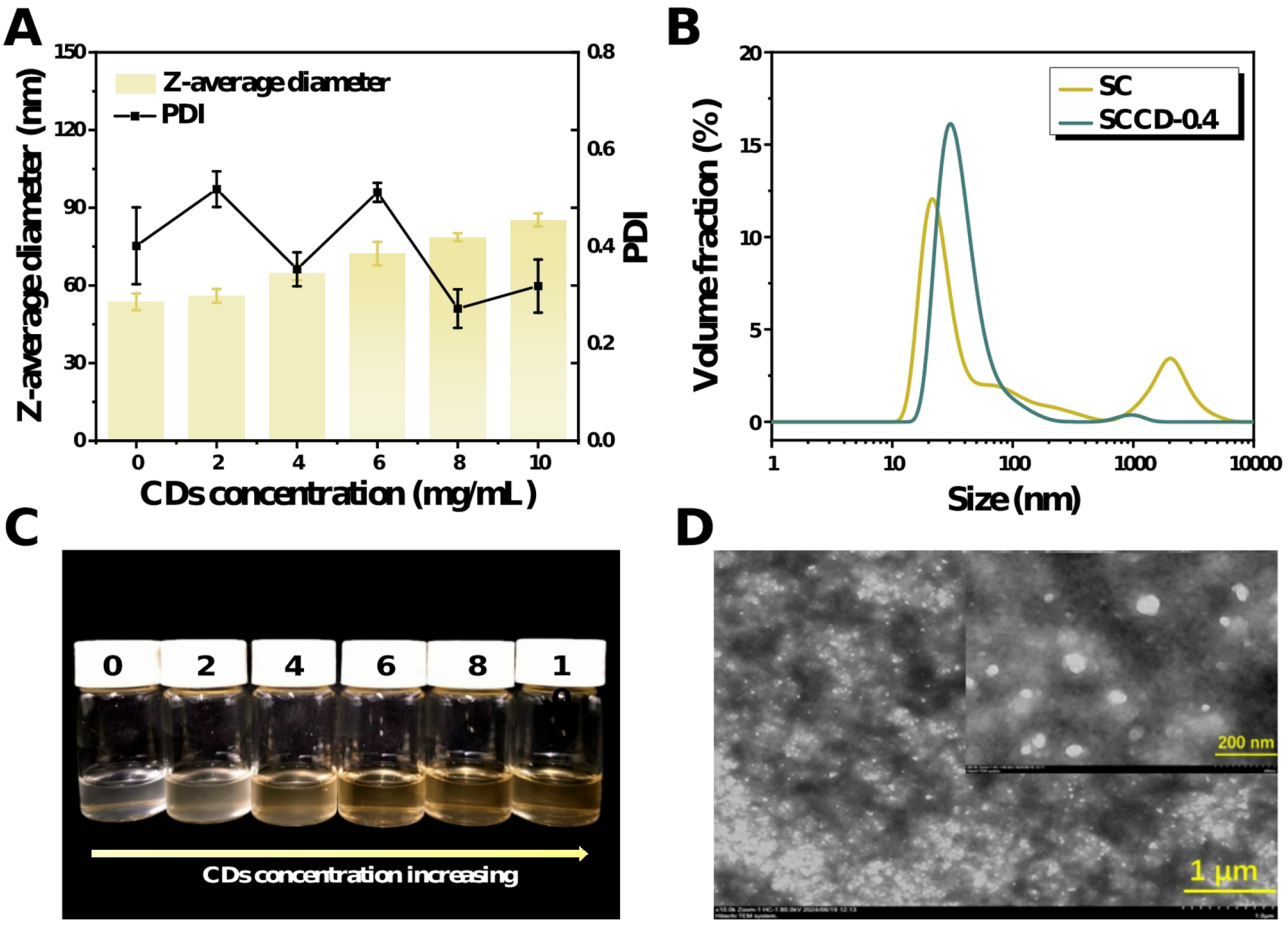

Fig. 2. (**A**) The z-average diameter and PDI of SCCD composite coating, (**B**) Size distribution of SC and SCCD-0.4, (**C**) Apparent diagram of SCCD composite coating, the concentration of CDs was 0 (SC), 2, 4, 6, 8 and 10 mg / mL from left to right, (**D**) TEM image of SCCD.

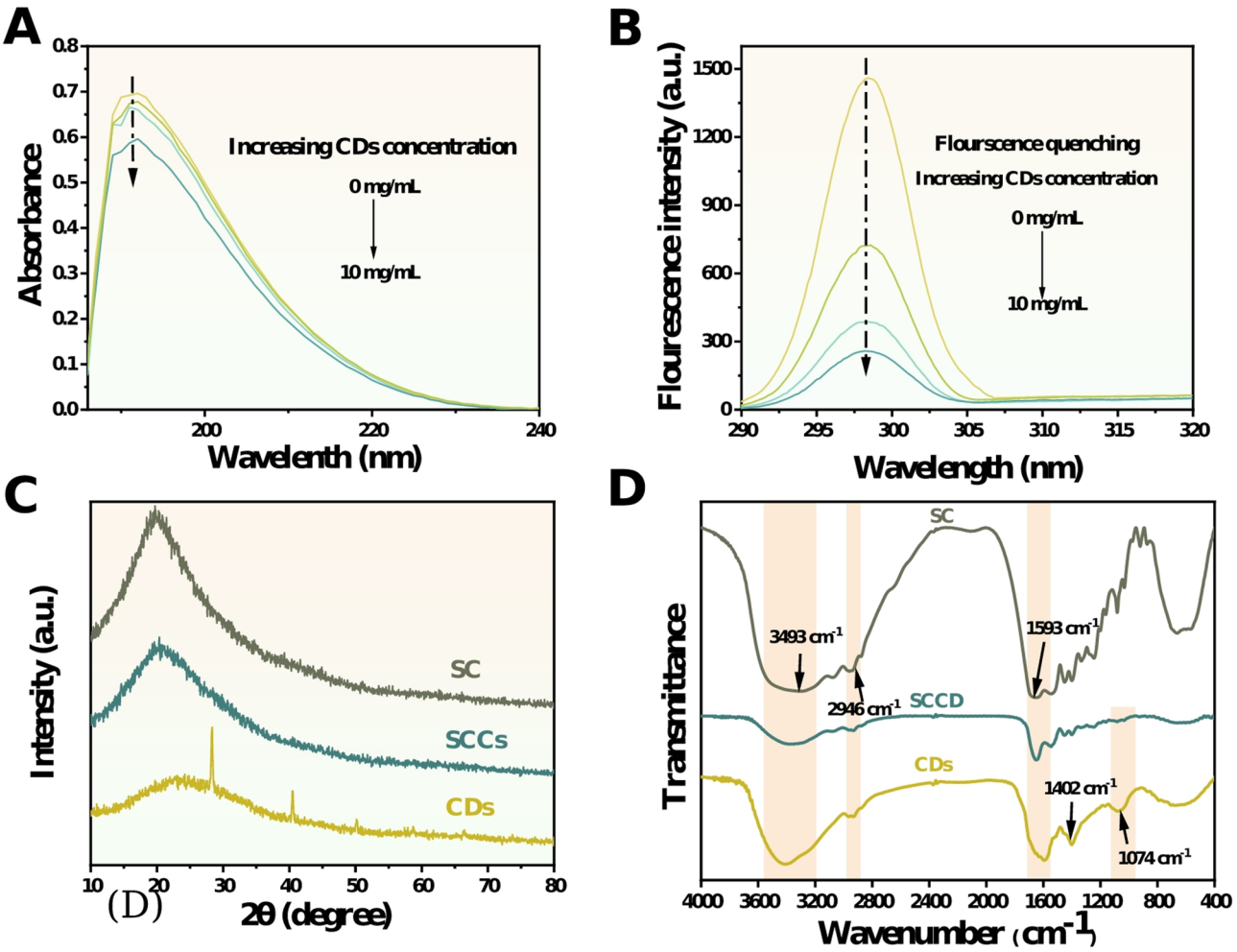

Fig. 3. (**A**) UV spectra spectroscopy, (**B**) Intrinsic fluorescence of SCCD coating, (**C**) XRD pattern and (**D**) FTIR spectrum of SC, SCCD, and CDs.

observed between 190 and 200 nm. Composite coatings with added CDs have a much lower absorption value, and this value continues to fall as the concentration of CDs increases.

Endogenous fluorescence quenching of proteins is a crucial analytical approach for analyzing the interaction between biological macromolecules and small molecules. It can be used to analyze the interaction between proteins and hydrophobic bioactive compounds[24]. As the concentrations of CDs grow from 0 to 10 mg/mL, the typical intrinsic fluorescence emission profiles of the protein are shown in Fig. 3B. Upon increasing concentration of CDs, the maximum fluorescence intensity progressively decreased, indicating that there was interaction between SC and CDs.

FTIR spectrum and XRD pattern was used to analyze the structural insights and surface state of SC, SCCD and CDs. As FTIR spectra show in Fig. 3D, the CDs presented abundant hydroxyl groups, such as 3407 cm^{-1} (V_{O-H}). Moreover, stretching vibrations were observed, such as 2946 cm^{-1}, 1402 cm^{-1}, 1074 cm^{-1} (V_{C-H}) and 1593 cm^{-1} ($V_{C=C}$). The FTIR spectrum of SCCD shows that the peaks shifted compared with the peaks from the spectrum of CDs and SC. By comparing the spectra of CDs and composite coating, it is found that SCCD composite coating and pure CDs showed very similar absorption peaks, which may be due to sericin protein being a good embedding material, which can highlight the characteristics of carbon quantum dots. The result also demonstrated that no new chemical bonds were formed in SCCD composite coating, which is consistent with the study result of Xu et al.[25]. Figure 3C illustrates how the XRD pattern exhibits a peak at 24.2° for CDs that match to the graphite crystal planes. Additionally, it was mentioned that the random coil and typical β-sheet structures are responsible for the peaks for SC at 19.7°[26]. In comparison to SC and CDs, the peak of SCCD at 21.3° shifted somewhat; however, the integration of CDs did not alter the structure of the sericin protein.

Antibacterial properties of the SCCD composite coating

The antibacterial activity of the SCCD coating against *E. coli* and *B. subtilis* is measured by Oxford-cup method, as shown in Fig. 4 and Table 1. Inhibition zone diameters against *E. coli* and *B. subtilis* with SCCD-1.0 were much larger than for SC. As seen from Table 1, the unit of the diameter is mm, in comparison to the SC, the antibacterial activity of SCCD-1.0 increased by 146% (for *B. subtilis*) and 157% (for *E. coli*), and the inhibition

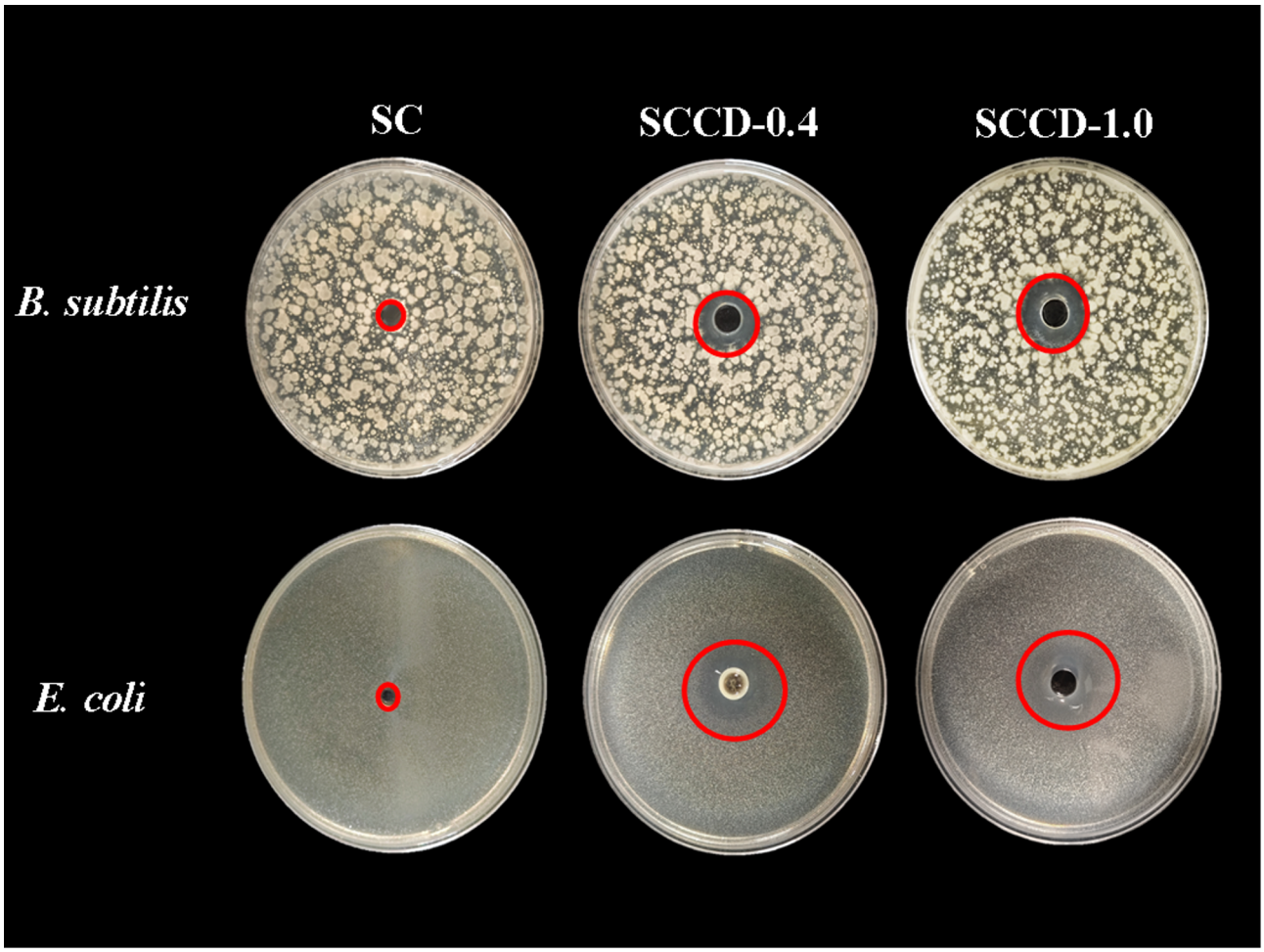

Fig. 4. The inhibition zone of SCCD coating against *B.subtilis* and *E.coli* with the concentration of CDs 0 mg/mL, 4 mg/mL, and 10 mg/mL in SC solution.

Bacterium	SC	SCCD-0.4	SCCD-1.0
B.subtilis	0.78	16.01 ± 0.026^{c}	19.21 ± 0.030^{b}
E.coli	0.78	19.63 ± 0.013^{a}	20.01 ± 0.062^{a}

Table 1. Inhibition zone diameters with different concentrations of SCCD against *B. subtilis* and *E. coli*. *The unit of the diameter is mm and ^{a,b,c} indicate significant difference ($p < 0.05$).

zones grew from 7.8 mm to 19.21 mm and 20.01 mm, respectively. The inhibition zone diameter of SCCD-1.0 was much larger than in other concentrations. This represents a significantly greater antimicrobial effect than observed with intermediate concentrations (SCCD-0.4 showed 16.01 mm and 19.63 mm inhibition zones for *B. subtilis* and *E. coli*, respectively). Because of the quantum size effect, CDs have more functional groups that contain oxygen, which increases the oxidative stress impact and kills bacteria[27]. CDs work in concert with a variety of pathways to have antibacterial activity. By diffusion and electrostatic action, CDs can be adsorbed to the bacterial cell walls in the dark. Bacteria become sequestered as a result, hindering their ability to absorb nutrients and interfering with their natural metabolism. When CDs penetrate a bacterial cell, they have the ability to attach to both DNA and RNA, changing the secondary conformation of the former and causing the separation of the DNA double helix. Bacterial cells eventually undergo apoptosis as a result of a number of factors working together, having an antibacterial impact.

The inhibition zone diameters for *B. subtilis* shown significant differences between SCCD-0.4 (16.01 ± 0.026 mm) and SCCD-1.0 (19.21 ± 0.030 mm), showing concentration-dependent antimicrobial activity, according to statistical analysis (one-way ANOVA with Tukey's post-hoc test, the different small letters indicate significant difference). The differences between SCCD-1.0 (20.01 ± 0.062 mm) and SCCD-0.4 (19.63 ± 0.013 mm) for *E. coli*, however, were not statistically significant, indicating that the bacteria was less sensitive to the concentration rise in these experimental settings. Gram-positive bacteria lack an outer

membrane, which makes them more vulnerable to some antibiotics that target the cell wall than gram-negative bacteria, while having a thicker peptidoglycan layer. In contrast, the cell wall of gram-negative bacteria is more complicated, with a thinner peptidoglycan layer and an outside phospholipid membrane. G^- bacteria are more effectively defended against by their outer phospholipid membrane.

Spinach preservation experiment

Effect of different coating packaging on the appearance of spinach

We can roughly judge the quality of spinach through observation. As shown in Fig. 5, with the prolongation of storage time, the leaves of spinach began to wilt and turn yellow in the fourth day with the unique fragrance disappearing. Then, the stems shift from firm and shaped which could be pinched with nails to soft and cracked. Fine lines appeared, indicating loss of water, mainly due to a series of chemical changes during storage affected the quality of spinach. According to Fig. 6A–D, we record the sensory evaluation index (appearance, odor, color, and texture) of spinach treated by different solutions during storage. There was not much variation of performance between the groups in the early two days. However, on the 4 d, the dehydration caused the spinach treated with SC to wilt fast, changing its color from a vibrant green to a dull green. After 6 d, there were significant differences in the indexes of the different treatments. Leaf edges in the group of CT and SC displayed yellowing and mild rot, and their texture softened and even reached an inedible state on the 8 d. Among four group, the CT group had the highest degree of decay and a higher degree of leaf curl aging, in contrast, the spinach in the control group treated with SCCD-1.0 sample solution had the best appearance. This phenomenon indicating that SCCD effectively delayed the spoilage and deterioration of the spinach.

Effect of different coating packaging activity on physiological and biochemical indicators in spinach

The weight loss rate is an important indicator to reflect the storage quality of leafy vegetables. The transpiration of the leaves after harvest and the water loss due to cutting and storage conditions (temperature and humidity) are the main reasons for the increase in mass loss. Figure 7A suggests that the weight loss of the experimental group treated with SCCD composite coating was significantly lower than that of the group of CT and SG, and

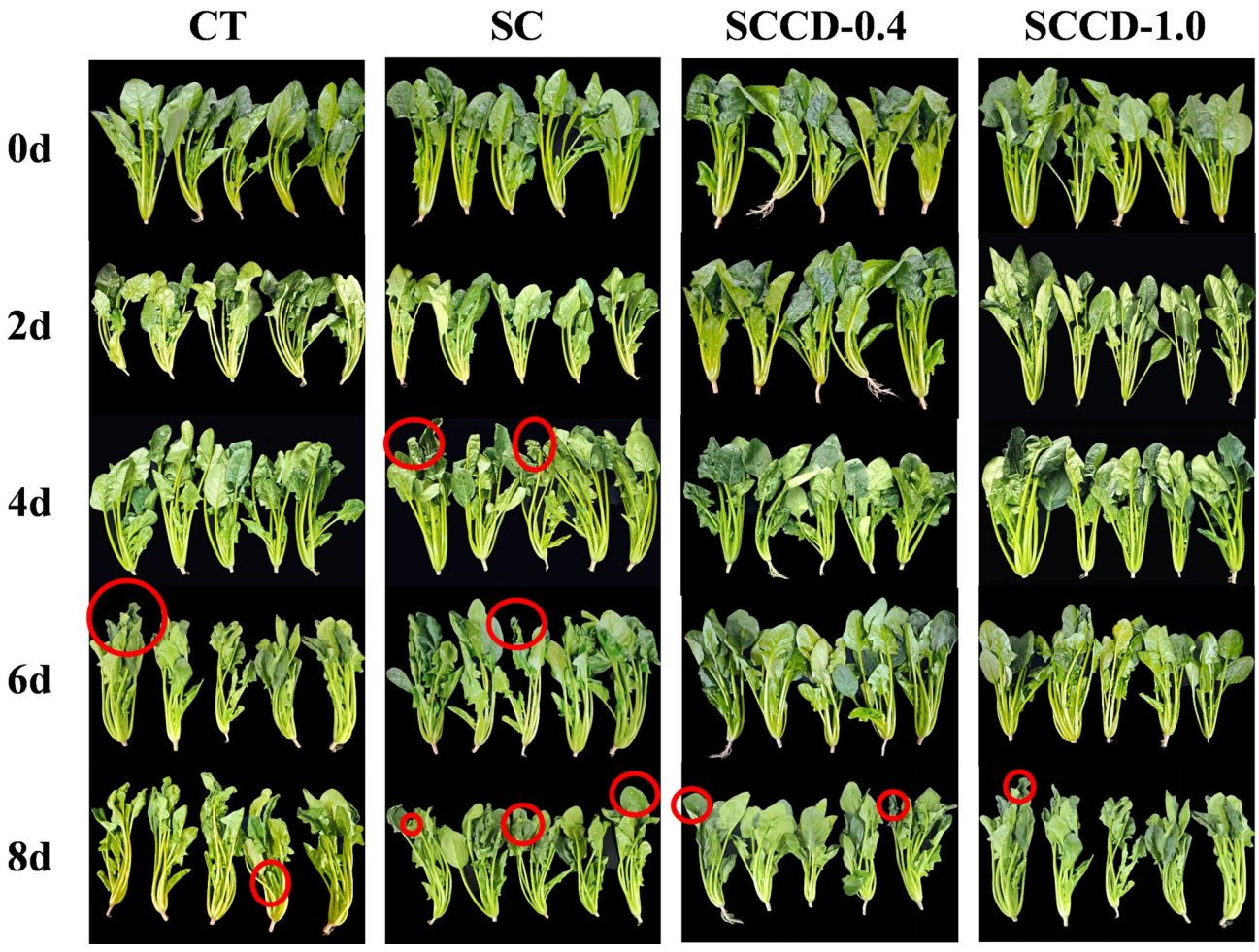

Fig. 5. Effects of different treatments (CT: Purified water; SC: 10 mg/mL sericin Protein solution; SCCD-0.4: contained 4 mg/mL CDs in sericin protein; SCCD-1.0: contained 10 mg/mL CDs in sericin protein) on the appearance and morphology of spinach during storage.

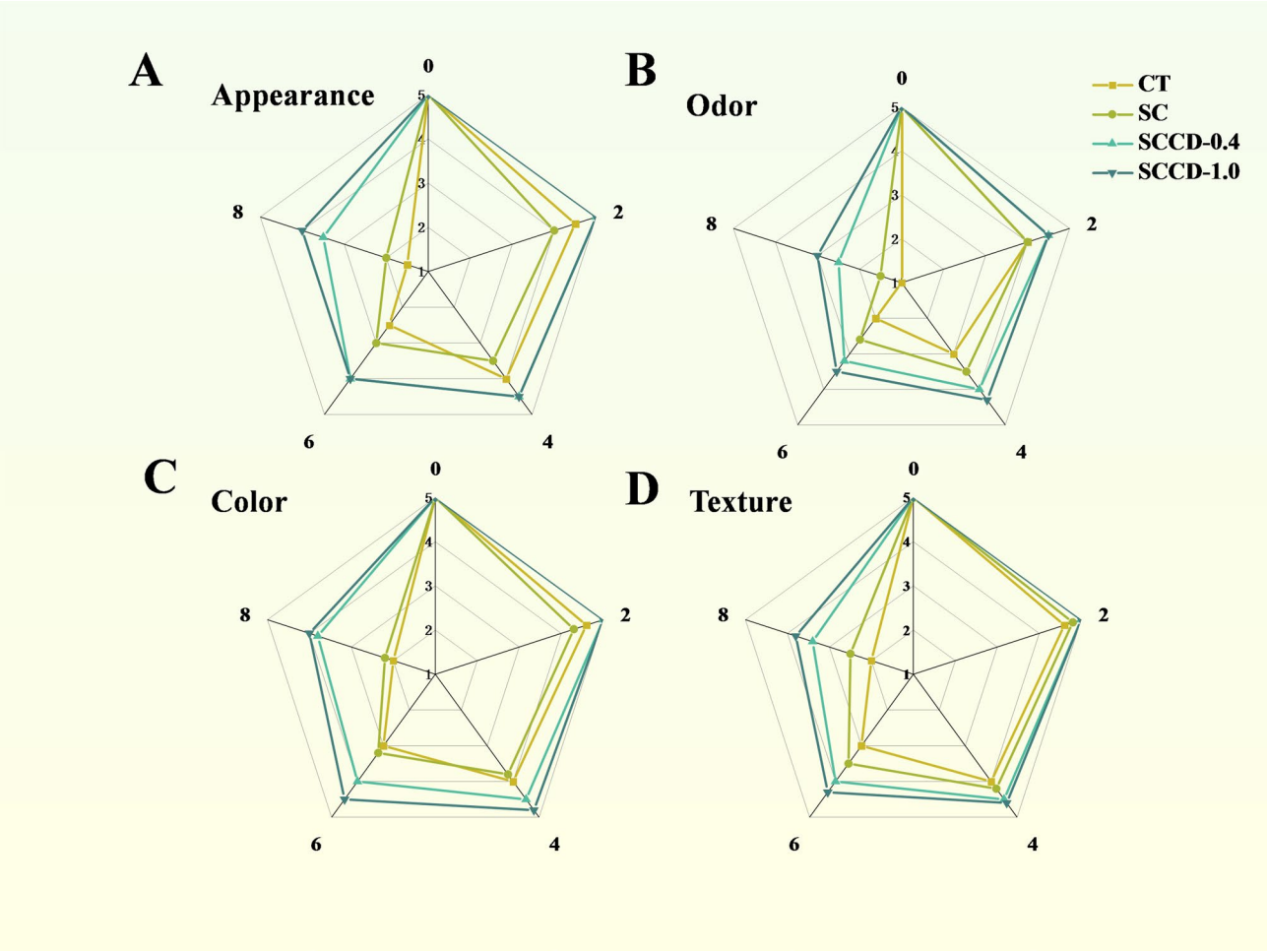

Fig. 6. Effects of SCCD coating on sensory evaluation of the (**A**) appearance, (**B**) odor, (**C**) color and (**D**) texture during storage.

the weight loss rate of group treated by SCCD-1.0 (3.56%) was obviously lower than that of SCCD-0.4 (5.84%). This can be attributed to the blocking effect of carbon point. With the increase of CDs concentration in SCCD composite coating, it can effectively block oxygen and water, slow down the respiration and transpiration of spinach, and maximize the quality of spinach. This consequence illustrated that SCCD coating can effectively postpone vegetables water and quality loss.

Oxidation is the major cause of food spoilage[28] and MDA is the main product of membrane lipid peroxidation which can directly poison cells, and its content is an important index to judge the damage degree of fruit and vegetable membrane system[29]. The final product of lipid peroxidation is MDA, the level of which directly reflects the degree of oxidative damage to the cell membrane, and the accumulation of MDA can also lead to enzymatic browning of fruits and vegetables. Figure 7B shows that as storage time increased, the MDA content in each experimental group rose as well, making the difference increasingly noticeable. The MDA content of all treated spinach increased after 8 d of storage, among which the MDA content of CT group was the highest (1.91 mol/g), followed by the SC material treatment group (1.45 mol/g), the SCCD-0.4 treatment group (0.83 mol/g), and the SCCD-1.0 packaging material treatment group (0.80 mol/g). On the 8 d, the CT group's MDA concentration was 2.39 times higher in the SCCD-1.0. In conclusion, the SCCD composite coating successfully reduced the rise in MDA content in spinach, thereby preventing oxidative damage to the sample's cell membrane. This is because the surface of CDs is rich in functional groups like hydroxyl groups (-OH) and carboxyl groups (-COOH), which can supply hydrogen atoms or electrons to play an antioxidant role, effectively preventing the formation of malondialdehyde as a peroxide.

Spinach contains a lot of chlorophyll to keep the leaves bright green in color, and chlorophyll degradation is a sign of the onset of leaf senescence, which is the result of chloroplast lipid peroxidation and thylakoid membrane degradation. As shown in Fig. 7C, with the increase of storage time, the chlorophyll content of each group decreased, and the chlorophyll content of the control group decreasing by 0.39 g/kg was the fastest, while the chlorophyll content of the experimental group treated with SCCD-0.4 was the highest 0.58 g/kg after 8 days of storage. In the middle, the SC treatment group (0.44 g/kg) and the SCCD-1.0 group (0.51 g/kg) were in order. The analysis showed that the low concentration of CDs coating had obvious advantages in inhibiting chlorophyll degradation and leaf yellowing. On the one hand, the carbon point uses its own structure to scavenge

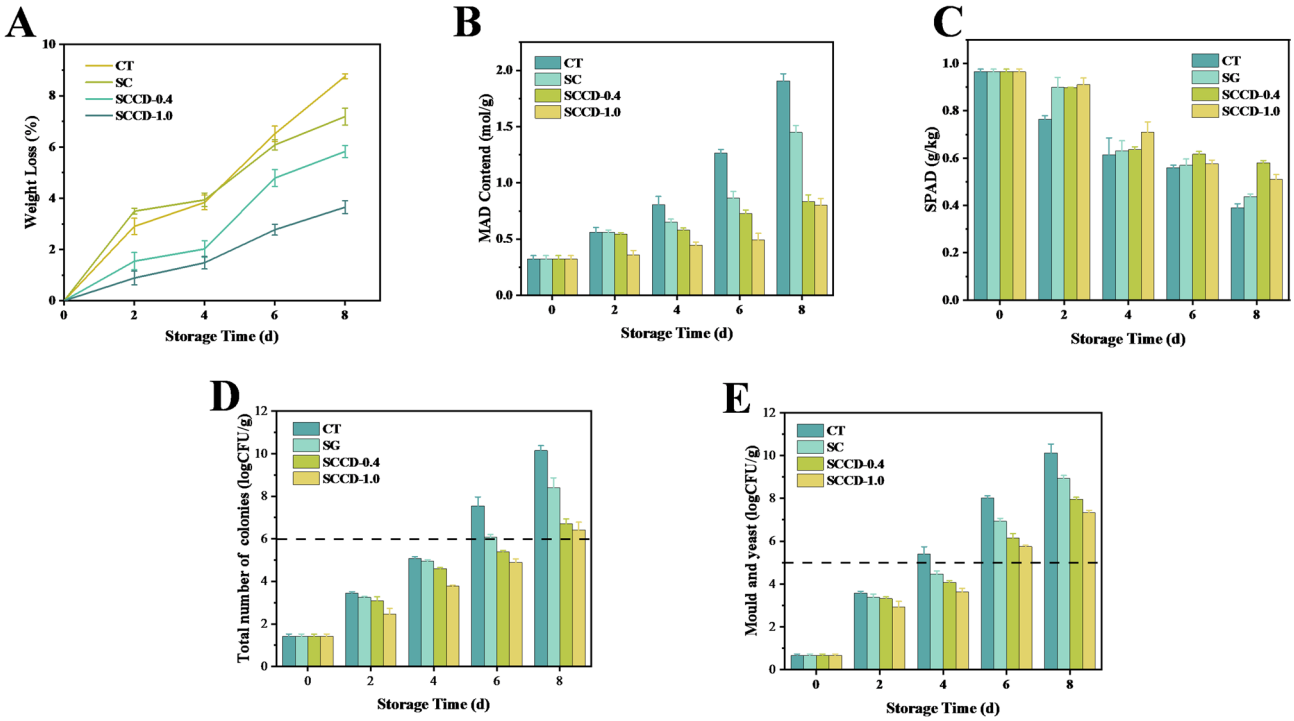

Fig. 7. Effect of SCCD coating on (**A**) weight loss, (**B**) MDA contends, (**C**) chlorophyll, (**D**) total number of colonies and (**E**) mold and yeast of spinach during storage time.

free radicals to inhibit the degradation of chlorophyll. On the other hand, the carbon point can interact with the chlorophyll molecular release to stabilize the structure of chlorophyll by forming hydrogen bonds and prevent its degradation during storage.

Bacteria, yeasts, molds and viruses will endanger food safety and are the main causes of fresh-cut product spoilage[30]. Microorganisms will decompose carbohydrates and proteins in vegetable substrates into lactic acid, ethanol, acetic acid, amino acids and other substances, and further generate ketones, aldehydes, alcohols, esters and other flavor substances. Therefore, the control of microbial contamination is essential for fresh-cut vegetables. Some western countries had formulated microbial safety standards for fresh-cut fruits and vegetables, in which the total number of colonies should be less than 10^5 CFU/g or 10^6 CFU/g[20]. Because carbon point has both a blocking effect and an antibacterial action that interferes with the metabolic processes of bacteria and fungi, it can effectively stop spoiling from external microorganisms. Figure 7D-E shows the total number of colonies and the number of molds and yeast of the control group surpassed the safety standards in after 6d and 4d respectively, while in spinach treated by SCCD composite coating it was 8d and 6d respectively. The SCCD composite coating treatment significantly reduced the total loads of studied microbes on the samples. Total aerobic mesophilic bacteria, molds and yeasts gradually increased during storage. Total counts of aerobic mesophilic bacteria for control, CT, SC, SCCD-0.4 and SCCD-1.0 on the 8th day of storage were 10.15, 8.40, 6.70, 6.42 log CFU/g, respectively. Total counts of molds and yeasts for control, CT, SC, SCCD-0.4 and SCCD-1.0 on the 8th day of storage were 10.12, 8.93, 7.67, 7.34 log CFU/g, respectively. From the observation in the figure, it can be seen that the composite coating has a certain effect on inhibiting the increase of microorganisms in fresh-cut vegetables and fruits.

Conclusion

In summary, we successfully added CDs to sericin to prepare the bio-composite coating with anti-counterfeiting, antibacterial, antioxidant, and UV shielding. The evaluation of various physiological and biochemical indices of spinach indicated that this coating packing treatment was successful in extending the shelf life of spinach by delaying mass loss, chlorophyll degradation, microbial growth and oxidation. Notably, the coating with the highest CDs contend (SCCD-1.0) has the most effective preservation effect on spinach. Furthermore, the fluorescence quenching and PDI data showed that the nanosuspension's distribution was uniform under the interaction of CDs and SC. These results show that the combination of SCCD may produce a low-cost and high-efficiency active packaging material, and have the potential to be applied to the preservation of postharvest vegetables.

Data availability

The data that support the findings of this study are available from the corresponding author Lingling Liu (E-mail: llliu@zust.edu.cn) upon reasonable request.

Received: 30 September 2024; Accepted: 17 June 2025
Published online: 11 July 2025

References

1. Luo, Z., Wang, Y., Wang, H. & Feng, S. Impact of nano- $CaCO_3$ -LDPE packaging on quality of fresh-cut sugarcane. *J. Sci. Food Agric.* **94**, 3273–3280 (2014).
2. Lo, C. H. et al. Association of Ultra-processed food and unprocessed or minimally processed food consumption with bowel habits among U.S. Adults. *Clin. Gastroenterol. Hepatol.* **22**, 2309–2318e5 (2024).
3. Mahardiani, L., Larasati, R., Susilowati, E., Hastuti, B. & Azizah, N. L. Potential edible coating of pectin obtained from banana peel for fruit preservation. *J. Phys. Conf. Ser.* **1912**, 012019 (2021).
4. De Oliveira Filho, J. G., Miranda, M., Ferreira, M. D. & Plotto, A. Nanoemulsions as edible coatings: A potential strategy for fresh fruits and vegetables preservation. *Foods* **10**, 2438 (2021).
5. Guo, B. et al. Multifunctional carbon dots reinforced gelatin-based coating film for strawberry preservation. *Food Hydrocoll.* **147**, 109327 (2024).
6. Wang, M. et al. Visible light-responsive chitosan/sodium alginate/QDs@ZIF-8 nanocomposite films with antibacterial and ethylene scavenging performance for Kiwifruit preservation. *Food Hydrocoll.* **145**, 109073 (2023).
7. Xin, Y., Yang, C., Zhang, J. & Xiong, L. Application of whey protein-based emulsion coating treatment in fresh-cut apple preservation. *Foods* **12**, 1140 (2023).
8. Hou, C. Y. et al. Effect of D-Limonene nanoemulsion edible film on banana (Musa sapientum Linn.) post-harvest preservation. *Molecules* **27**, 6157 (2022).
9. Mei, S. et al. Developing silk sericin-based and carbon dots reinforced bio-nanocomposite films and potential application to litchi fruit. *LWT* **164**, 113630 (2022).
10. Seo, S. J., Das, G., Shin, H. S. & Patra, J. K. Silk sericin protein materials: Characteristics and applications in food-sector industries. *Int. J. Mol. Sci.* **24**, 4951 (2023).
11. Xu, X. et al. Electrophoretic analysis and purification of fluorescent single-walled carbon nanotube fragments. *J. Am. Chem. Soc.* **126**, 12736–12737 (2004).
12. Wang, Y., Qiu, W., Fang, X., Li, W. & Sun, Y. Carbon dots-based reinforced hydrogen-rich water nanocomposite coating for storage quality of fresh-cut Pear. *Food Biosci.* **53**, 102837 (2023).
13. Du, H. & He, L. Synergistic improvement of antioxidant and antibacterial properties of carbon quantum complexes with zinc doping and chlorogenic acid for Longan preservation. *Food Chem.* **439**, 138169 (2024).
14. Fan, K., Zhang, M., Fan, D. & Jiang, F. Effect of carbon dots with chitosan coating on microorganisms and storage quality of modified-atmosphere-packaged fresh-cut cucumber. *J. Sci. Food Agric.* **99**, 6032–6041 (2019).
15. Zheng, Y., Li, L., Shen, H., Chen, C. & Xie, J. Preparation of slow-release polylactic acid antibacterial active packaging films and its application in spinach preservation. *Food Bioprocess. Technol.* **18**, 1346–1364 (2025).
16. Sul, Y., Ezati, P. & Rhim, J. W. Preparation of chitosan/gelatin-based functional films integrated with carbon dots from banana peel for active packaging application. *Int. J. Biol. Macromol.* **246**, 125600 (2023).
17. Liu, L. et al. High-performance films fabricated by food protein nanofibrils loaded with vanillin: Mechanism, characterization and bacteriostatic effect. *Food Packag Shelf Life*. **37**, 101080 (2023).
18. Patil, A. S. et al. Photophysical insights of highly transparent, flexible and re-emissive PVA @ WTR-CDs composite thin films: A next generation food packaging material for UV blocking applications. *J. Photochem. Photobiol Chem.* **400**, 112647 (2020).
19. Zhou, W. et al. Fabrication of caseinate stabilized thymol nanosuspensions via the pH-driven method: Enhancement in water solubility of thymol. *Foods* **10**, 1074 (2021).
20. Liu, L. et al. pH-driven formation of soy protein isolate-thymol nanoparticles for improved the shelf life of fresh-cut lettuce. *Food Control*. **160**, 110306 (2024).
21. Chen, L. & Fan, K. Influence of ultrasound treatment in combination with modified atmosphere on microorganisms and quality attributes of fresh-cut lettuce. *Int. J. Food Sci. Technol.* **56**, 5242–5249 (2021).
22. Wang, M. et al. Development of packaging films based on UiO-66 MOF loaded melatonin with antioxidation functions for spinach preservation. *Food Chem.* **440**, 138211 (2024).
23. Zhao, L., Zhang, M., Mujumdar, A. S., Adhikari, B. & Wang, H. Preparation of a novel carbon dot/polyvinyl alcohol composite film and its application in food preservation. *ACS Appl. Mater. Interfaces*. **14**, 37528–37539 (2022).
24. Zu, F. et al. The quenching of the fluorescence of carbon dots: A review on mechanisms and applications. *Microchim Acta*. **184**, 1899–1914 (2017).
25. Xu, L. et al. Preparation and performance of radiata-pine-derived polyvinyl alcohol/carbon quantum dots fluorescent films. *Materials* **13**, 67 (2020).
26. Fu, Z. et al. Construction and biocompatibility evaluation of fibroin/sericin-based scaffolds. *ACS Biomater. Sci. Eng.* **8**, 1494–1505 (2022).
27. Kousheh, S. A., Moradi, M., Tajik, H. & Molaei, R. Preparation of antimicrobial/ultraviolet protective bacterial nanocellulose film with carbon dots synthesized from lactic acid bacteria. *Int. J. Biol. Macromol.* **155**, 216–225 (2020).
28. Fu, B. et al. Carbon dots enhanced gelatin/chitosan bio-nanocomposite packaging film for perishable foods. *Chin. Chem. Lett.* **33**, 4577–4582 (2022).
29. Wantat, A., Seraypheap, K. & Rojsitthisak, P. Effect of chitosan coatings supplemented with chitosan-montmorillonite nanocomposites on postharvest quality of 'hom thong' banana fruit. *Food Chem.* **374**, 131731 (2022).
30. Huang, H. et al. UV-C treatment affects browning and starch metabolism of minimally processed Lily bulb. *Postharvest Biol. Technol.* **128**, 105–111 (2017).

Acknowledgements

This research was funded by National Key Research and Development Program of China-Intergovernmental Cooperation Project (No.2024YFE0197800), Hainan Province Science and Technology Special Fund (No. GHYF2025035), Basic Scientiffc Research Project of Zhejiang University of Science and Technology (No. 2025QN036), the Scientific Research Project of Zhejiang Provincial Department of Education (No. Y202454700) and the Major Scientific Research Achievement Transformation Project of Ningxia Hui Autonomous Region (No. 2023CJE09060).

Author contributions

S.Z. and L.J. wrote the main manuscript, with Y.Z. preparing Figures. F.C. supervised and conducted formal analysis. A.F. handled data validation and curation. T. Y. provided resources and software. G. Y. conducted formal analysis. Z. B. oversaw administration and funding. L. L. conceptualized, drafted the manuscript, and contributed to methodology, resources, and validation.All authors reviewed the manuscript.

Declarations

Competing interests
The authors declare no competing interests.

Additional information
Correspondence and requests for materials should be addressed to L.L.

Reprints and permissions information is available at www.nature.com/reprints.

Publisher's note Springer Nature remains neutral with regard to jurisdictional claims in published maps and institutional affiliations.

Open Access This article is licensed under a Creative Commons Attribution-NonCommercial-NoDerivatives 4.0 International License, which permits any non-commercial use, sharing, distribution and reproduction in any medium or format, as long as you give appropriate credit to the original author(s) and the source, provide a link to the Creative Commons licence, and indicate if you modified the licensed material. You do not have permission under this licence to share adapted material derived from this article or parts of it. The images or other third party material in this article are included in the article's Creative Commons licence, unless indicated otherwise in a credit line to the material. If material is not included in the article's Creative Commons licence and your intended use is not permitted by statutory regulation or exceeds the permitted use, you will need to obtain permission directly from the copyright holder. To view a copy of this licence, visit http://creativecommons.org/licenses/by-nc-nd/4.0/.

© The Author(s) 2025